Radar-Based Over-The-Air Message Generator for Accelerating Connected Vehicle Deployment

CONNECTED VEHICLE/INFRASTRUCTURE UNIVERSITY TRANSPORTATION CENTER (CVI-UTC)

MORGAN STATE UNIVERSITY

VirginiaTech Transportation Institute

UNIVERSITY of VIRGINIA

VDOT

Radar-Based Over-the-Air Message Generator for Accelerating Connected Vehicle Deployment

Prepared for the Research and Innovative Technology Administration (RITA); U.S. Department of Transportation (US DOT)

Grant Project Title:
Advanced Operations Focused on Connected Vehicles/Infrastructure (CVI-UTC)

Consortium Members:
Virginia Tech Transportation Institute (VTTI),
University of Virginia (UVA) Center for Transportation Studies,
and Morgan State University (MSU).

Program Director:
Dr. Thomas Dingus
Program Director, Connected Vehicle/Infrastructure
University Transportation Center
Director, Virginia Tech Transportation Institute
Professor, Department of Biomedical Engineering and Mechanics
at Virginia Tech
tdingus@vtti.vt.edu
(540) 231–1501

Report Authors:
Reginald Viray
Research Associate, Center for Advanced Automotive Research
Virginia Tech Transportation Institute
rviray@vtti.vt.edu
(540) 231-1500

Thomas Gorman
Research Associate, Center for Advanced Automotive Research
Virginia Tech Transportation Institute
tgorman@vtti.vt.edu
(540) 231-1500

Zac Doerzaph
Director, Center for Advanced Automotive Research
Virginia Tech Transportation Institute
zdoerzaph@vtti.vt.edu
(540) 231-1046

DUNS: 0031370150000 EIN: 54-6001805

Grant Funding Period: January 2012 – November 2016
Final Research Reports

October 15, 2016

Disclaimer

The contents of this report reflect the views of the authors, who are responsible for the facts and the accuracy of the information presented herein. This document is disseminated under the sponsorship of the U.S. Department of Transportation's University Transportation Centers Program, in the interest of information exchange. The U.S. Government assumes no liability for the contents or use thereof.

Connected Vehicle/Infrastructure UTC

The mission statement of the Connected Vehicle/Infrastructure University Transportation Center (CVI-UTC) is to conduct research that will advance surface transportation through the application of innovative research and using connected-vehicle and infrastructure technologies to improve safety, state of good repair, economic competitiveness, livable communities, and environmental sustainability.

The goals of the Connected Vehicle/Infrastructure University Transportation Center (CVI-UTC) are:

- Increased understanding and awareness of transportation issues
- Improved body of knowledge
- Improved processes, techniques and skills in addressing transportation issues
- Enlarged pool of trained transportation professionals
- Greater adoption of new technology

Abstract

The market penetration levels needed to realize the full safety, economic, and environmental benefits of connected vehicle (CV) systems will not be met for some time. During the transition, it would be beneficial if data on non-CVs could be measured and included within the real-time CV data stream. Conceptually, a connected vehicle with advanced sensors, such as radar, could measure the dynamics of adjacent vehicles and, in addition to broadcasting its own Basic Safety Message (BSM), broadcast a pseudo BSM representing the non-connected vehicles.

This project investigated the use of radar sensors to compute the position, speed, and heading of a non-connected vehicle (non-CV) for packaging into a pseudo BSM. An algorithm was developed to estimate the speed, position, and heading of a nearby non-CV via speed, Global Positioning System (GPS) coordinates, and radar data from the CV. Field tests were conducted with two vehicles on the Virginia Smart Road and on public roads in the New River Valley of Virginia. The field tests were designed to cover a variety of vehicle formations, traffic densities, velocities, and roadway environments. The final results showed that 67.9% of the position estimates were within 3 m of the measured position along the *x*-axis (longitudinal) and within 1.5 m of the measured position along the *y*-axis (lateral). Heading and speed estimates were generally excellent. Although the estimated position accuracy was lower than desired, the data that were collected and analyzed were sufficient to suggest ways to improve the system, such as fusing the radar data with camera-based vision data or using a more accurate GPS.

Acknowledgements

The authors would like to thank the U.S. Department of Transportation – Research and Innovative Technology Administration, the University Transportation Centers Program, and the Virginia Tech Transportation Institute for funding this project. In addition, the support and skill set provided by the Center for Technology Development at the Virginia Tech Transportation Institute proved instrumental in the execution of this research project. The authors would like to thank Jean Paul Talledo Vilela, Joshua Quesenberry, Jacob Dennis, Tammy Russell, Andy Petersen, Arnab Gupta, Zeb Bowden, Melissa Hulse, and Leslie Harwood for their assistance in the various phases of this study. It should be noted that this document should be considered a technical report and has not been peer-reviewed for the purposes of publication.

Table of Contents

Background 1
Objectives 2
Method 2
System Architecture Development 3
Algorithm Development 3
Description of GHV sensor data 3
Coordinate Systems used in Algorithm Development 4
Algorithm Development for an Ideal System 6
Algorithm Development for a Realistic System 8
Vehicle System Development and Integration 9
Experimental Test Development and Execution 12
Smart Road Testing 12
Results 21
Algorithm Development Results for an Ideal System 22
Discussion 29
Conclusions and Recommendations 30
References 31

List of Figures

Figure 1. Limited CV environment characteristic of early stages of deployment. 1

Figure 2. Detection of Non-CVs by ranging sensor. 2

Figure 3. Connected sensor sharing. 2

Figure 4. Methodology workflow. 3

Figure 5. System concept. 3

Figure 6. Relationship between Geodetic, ECEF, and ENU coordinate systems. 5

Figure 7. Relationship between ENU and body-fixed coordinate systems. 6

Figure 8. Steps to calculate RV BSM measurements in ideal system. 7

Figure 9. Times at which measurements are made onboard the GHV. 9

Figure 10. System diagram. 10

Figure 11. Hirschmann shark fin combined DSRC/GPS antenna. 12

Figure 12. Segment of the Smart Road used for static dwell test. 13

Figure 13. Static dwell test. 14

Figure 14. Segment of the Smart Road used for dynamic ranging test. 14

Figure 15. Dynamic ranging test. 15

Figure 16. Smart Road course for dynamic platoon test. 16

Figure 17. Dynamic platoon test. 17

Figure 18. RV ahead cut-in scenario. 17

Figure 19. RV acceleration/deceleration test. 18

Figure 20. RV overtake test. 20

Figure 21. Route used for road testing (source:). 21

Figure 22. Comparison of actual RV measures against estimated RV measures. 23

Figure 23. Difference between actual RV measures and estimated RV measures. 24

Figure 24. Euclidean distances (in meters) between measured and estimated RV positions, projected onto axes of the GHV body-fixed coordinate system plotted against time. 25

Figure 25. Frequencies of binned Euclidean distances (in meters) between measured and estimated RV positions, projected onto axes of the GHV body-fixed coordinate system. 26

Figure 26.Euclidean distances (in meters) between measured and estimated positions, projected onto the *x*-axis, *y*-axis, and *z*-axis of the GHV body-fixed coordinate system plotted against the GHV measured radar range. 27

Figure 27. Estimates for radar misalignment as a function of radar range. 28

Figure 28. Frequencies of binned Euclidean distances (after radar misalignment correction) between measured and estimated RV positions, projected onto axes of the GHV body-fixed coordinate system..... 29

List of Tables

Table 1. OBE Technical Specifications (Savari 2012) 11

Table 2. BSM Data Elements (SAE International 2009)..... 11

Background

When connected vehicles (CVs) are initially deployed, the benefits of the system may not be readily available. Considering that the average lifespan of vehicles in the United States is approximately 15 years (National Highway Traffic Safety Administration, 2006), it will take time for the market penetration of CVs to reach the point where the system's potential can be fully realized. Even if all new vehicles are mandated to include such systems and aftermarket devices are available, a disproportionate ratio of non-CVs to CVs will be on the road for some time and legacy vehicles (e.g. collector cars) may be on the road indefinitely.

Since few CVs will be deployed initially, the CV environment will be incomplete in terms of data available for applications. This issue is illustrated in Figure 1, where only 2 out of 15 vehicles have a CV system. From a CV system standpoint, only the two CVs and connected infrastructure are aware of each other, and they have no knowledge of the other 13 vehicles on the roadway.

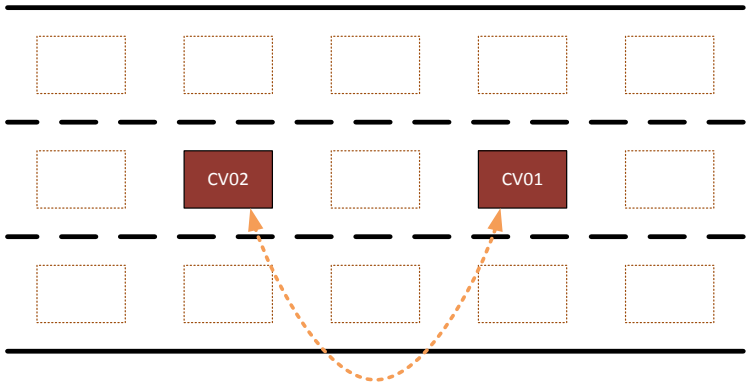

Figure 1. Limited CV environment characteristic of early stages of deployment.

To overcome this problem, ranging sensors, which are now becoming increasingly common in new vehicles, can be used. Data from these sensors can determine the relative distances to and speeds of other objects in the environment (Figure 2). As depicted in the figure, the Generating Host Vehicle (GHV) is the vehicle that contains equipment to detect and communicate the position of the other vehicles or Remote Vehicles (RV) in the roadway. This information can then be packaged into a CV system message, such as a Basic Safety Message (BSM) (SAE International, 2009), and then transmitted over-the-air (OTA) by a GHV for use by other CVs or infrastructure applications.

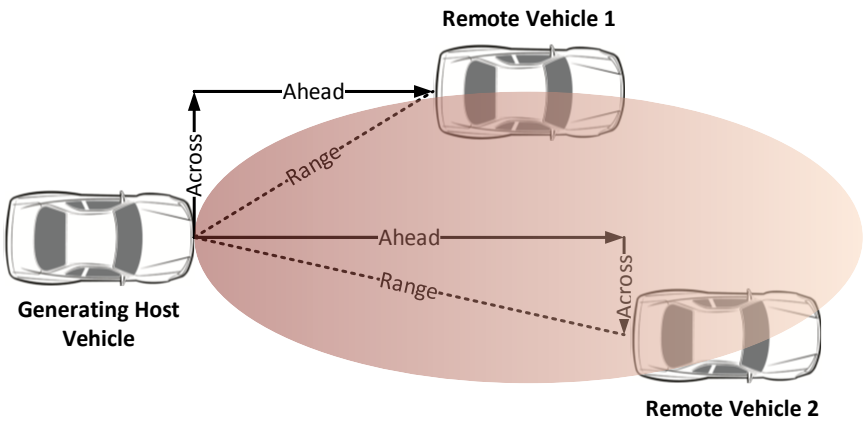

Figure 2. Detection of non-CVs by ranging sensor.

Figure 3 depicts an ideal situation where two GHVs with 360-degree sensor views are able to detect and share information about non-CVs. Figure 3 shows the same early deployment scenario as Figure 1, with two CVs and 13 non-CVs on the road. However, by utilizing ranging sensors the two CVs in Figure 3 are able to detect and report the non-CVs as remote vehicles (RVs), thus potentially improving the system's effectives during the early stages deployment.

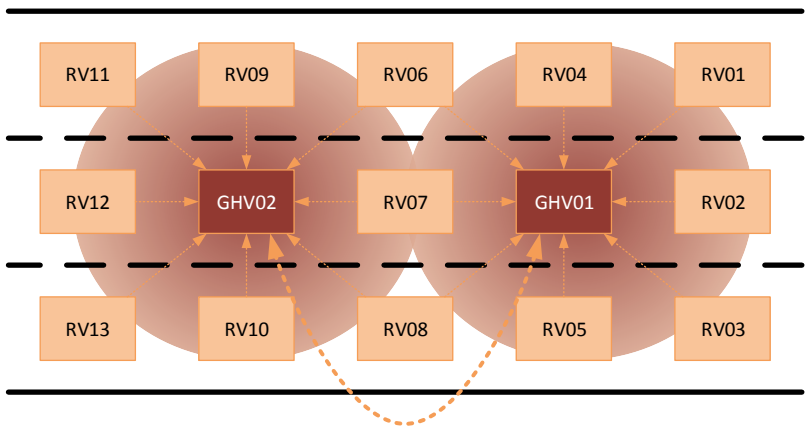

Figure 3. Connected sensor sharing.

Objectives

The primary objective of this project was to develop a technical implementation that will generate the position, speed, heading, and other Global Positioning System (GPS) elements of an RV target that can be used in OTA communications.

Method

Figure 4 displays the workflow implemented to meet the project's objectives. Details regarding the work performed in each block are provided below.

Figure 4. Methodology workflow.

System Architecture Development

Figure 5 shows a high-level systems diagram of the primary components required to develop an algorithm for estimating the GPS elements of a non-CV. This figure displays the integration and flow of information from hardware and software sources that will satisfy the algorithmic implementation. Details surrounding the components are described in subsequent sections.

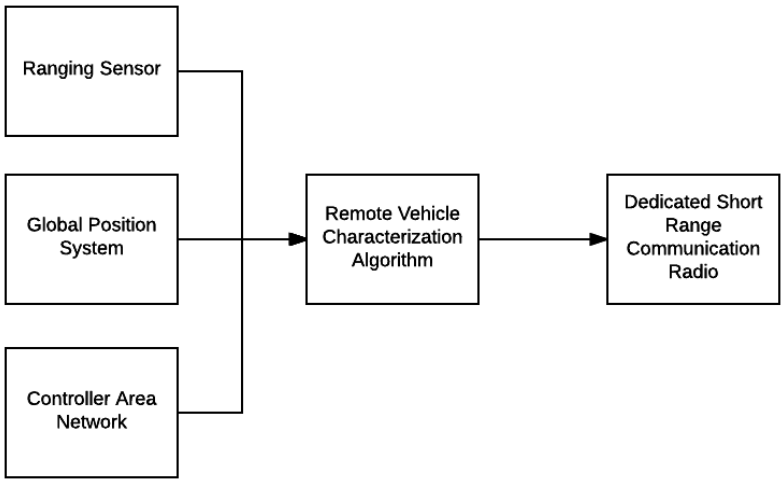

Figure 5. System concept.

Algorithm Development

Description of GHV Sensor Data

The objective of this project was to estimate the position, speed, and heading of at least one RV using measurements acquired onboard a GHV. GHV measurements were derived from three different systems.

The GPS receiver on the GHV measured the latitude, longitude, elevation, and heading of the GHV. The GHV's speed was collected directly from the Controller Area Network (CAN). Forward-facing radar captured data for up to eight different targets including:

- x_range – The distance between the GHV's front bumper and the RV's rear bumper projected onto the *x*-axis of the vehicle body-fixed coordinate system. x_range is the length of the "ahead" vector in Figure 2.

- y_range – The distance between the GHV's front bumper and the RV's rear bumper projected onto the *y*-axis of the vehicle body-fixed coordinate system. y_range is the length of the "across" vector in Figure 2.

- x_range_rate – The relative speed between the GHV's front bumper and the RV's rear bumper projected onto the *x*-axis of the vehicle body-fixed coordinate system.

- y_range_rate – The relative speed between the GHV's front bumper and the RV's rear bumper projected onto the *y*-axis of the vehicle body-fixed coordinate system.

- Object_ID – This variable is a counter that is used to track radar targets. Each time the radar system identifies a new target, the radar system assigns that target with a unique identifier.

Coordinate Systems used in Algorithm Development

The algorithms developed for this study relied on four coordinate systems:

- Geodetic

- Earth-Centered, Earth-Fixed (ECEF)

- East North Up (ENU)

- A body-fixed system centered on the vehicle

The Geodetic system describes position in terms of latitude (ϕ), longitude (λ), and elevation. The ECEF coordinate system is a three-dimensional Cartesian coordinate system with the origin fixed at the center of the Earth. The ENU coordinate system is a three-dimensional Cartesian coordinate system with its origin specified by a latitude and longitude. The relationship between the Geodetic, ECEF, and ENU coordinate systems is shown in Figure 6.

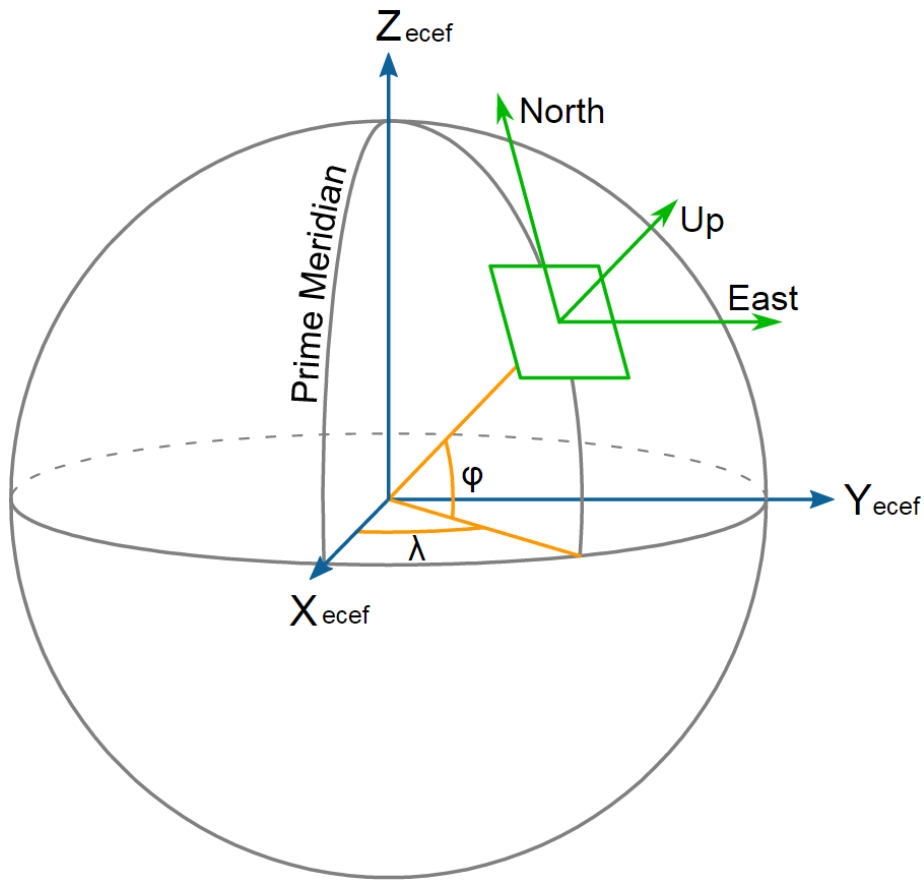

Figure 6. Relationship between Geodetic, ECEF, and ENU coordinate systems.

The GPS reported the GHV's position using the Geodetic system. GHV measurements were also made in the ENU and body-fixed coordinate systems. However, since calculation is easiest in the ECEF system, an integral part of the algorithm involved converting from one coordinate system to another.

Geodetic coordinates can be converted to ECEF coordinates using Equations 1 through 3.

$$X_{ecef} = (N + elevation)\cos(latitude)\cos(longitude) \tag{1}$$

$$Y_{ecef} = (N + elevation)\cos(latitude)\sin(longitude) \tag{2}$$

$$Z_{ecef} = (N * (1 - e^2) + elevation)\sin(latitude), \tag{3}$$

where *a* is the semi-major axis of the earth, *e* is the first numerical eccentricity of the earth, and

$$N = \frac{a}{\sqrt{1 - e^2 \sin^2(latitude)}}. \tag{4}$$

This study utilized Borkowski's Iterative Method (Burtch, 2006) to convert ECEF coordinates to GPS coordinates and rotation matrices to map the orientation of a vehicle from one Cartesian

coordinate system to another. The transformation from an ENU frame to the ECEF frame is given by Equation 5. The transformation from the ECEF frame to the ENU frame is the inverse (or transpose) of the same matrix.

$$R_{ENU\ to\ ECEF} = \begin{bmatrix} -\sin(\lambda) & -\cos(\lambda)\sin(\varphi) & \cos(\lambda)\cos(\varphi) \\ \cos(\lambda) & -\sin(\lambda)\sin(\varphi) & \sin(\lambda)\cos(\varphi) \\ 0 & \cos(\varphi) & \sin(\varphi) \end{bmatrix} \tag{5}$$

Figure 7 shows the relationship between an ENU frame and the vehicle body-fixed frame. The two frames are related by the heading of the vehicle, θ, which is measured by the GHV's GPS system.

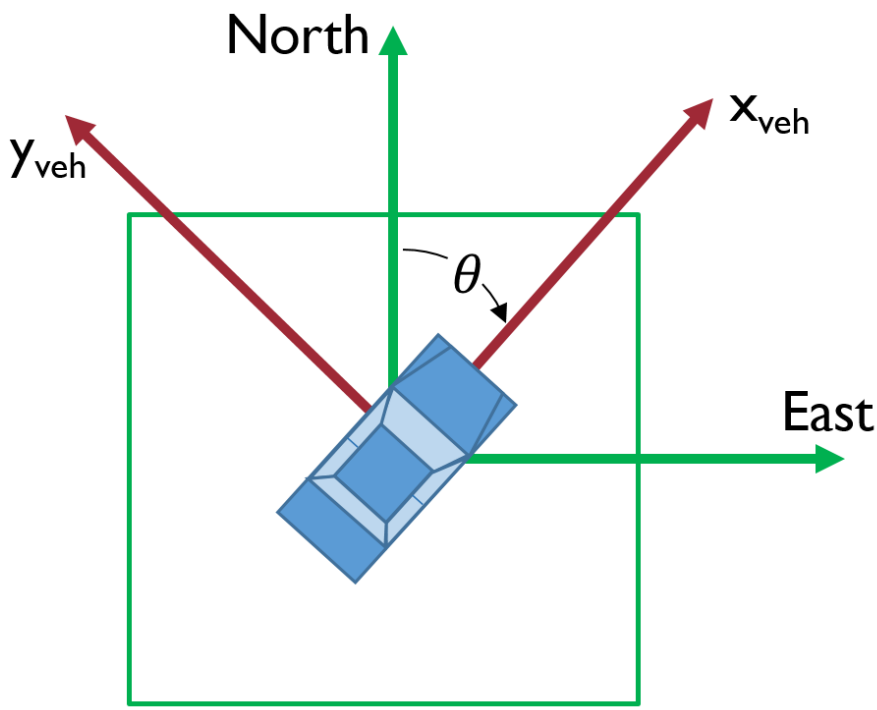

Figure 7. Relationship between ENU and body-fixed coordinate systems.

The transformation from the body-fixed frame to an ENU frame is given by Equation 6. The transformation from an ENU frame to the body-fixed frame is given by the inverse (or transpose) of the same matrix.

$$R_{body-fixed\ to\ ENU} = \begin{bmatrix} \sin(\theta) & -\cos(\theta) & 0 \\ \cos(\theta) & \sin(\theta) & 0 \\ 0 & 0 & 1 \end{bmatrix} \tag{6}$$

Algorithm Development for an Ideal System

The ideal system would be one in which the GHV's speed, GPS position, heading, and radar data would be sampled at the same frequency and aligned in time. Furthermore, an ideal system would be characterized by negligible error in these measurements. These ideal conditions provided a starting point for algorithm development.

An RV's GPS coordinates, speed, and heading can be computed using the GHV's GPS coordinates, speed, heading, and radar system through the five steps shown in Figure 8.

Figure 8. Steps to calculate RV BSM measurements in ideal system.

The first step is to compute the GHV's position in ECEF coordinates, which is accomplished using Equations 1 through 3. The second step is to determine the orientation of the GHV in ECEF coordinates. To be more specific, the algorithm calculates the unit vectors of the body-fixed coordinates mapped onto the ECEF coordinate system. The body-fixed *x*-coordinate unit vector (i.e., the GHV's heading) represented in ECEF coordinates is computed with Equation 7.

$$X_{body\ in\ ECEF} = R_{ENU\ to\ ECEF} * R_{body-fixed\ to\ ENU} \begin{bmatrix} 1 \\ 0 \\ 0 \end{bmatrix} \tag{7}$$

The body-fixed *y*-coordinate unit vector represented in ECEF coordinates is computed with Equation 8.

$$Y_{body\ in\ ECEF} = R_{ENU\ to\ ECEF} * R_{body-fixed\ to\ ENU} \begin{bmatrix} 0 \\ 1 \\ 0 \end{bmatrix} \tag{8}$$

The third step is to create a 6 × 1 vector that represents the kinematic state of the GHV, X_{HV}. The kinematic state is composed of the position and velocity of the GHV in ECEF coordinates. The vector is calculated using Equation 9.

$$X_{HV} = \begin{bmatrix} X_{ecef} \\ Y_{ecef} \\ Z_{ecef} \\ \text{speed} * X_{body\ in\ ECEF} \end{bmatrix} \tag{9}$$

The fourth step is to compute the kinematic state of the RV in ECEF coordinates. This step is accomplished with Equation 10. Note that $length_{veh}$ is the length of the GHV from the rear bumper to the front bumper. This correction is necessary because the radar system measures from bumper to bumper instead of from GPS unit to GPS unit.

$$X_{RV} = X_{HV} + \begin{bmatrix} (length_{veh} + radar\ x\ range) * X_{body\ in\ ECEF} \\ (radar\ x\ range\ rate) * X_{body\ in\ ECEF} \end{bmatrix} + \begin{bmatrix} (radar\ y\ range) * Y_{body\ in\ ECEF} \\ (radar\ y\ range\ rate) * Y_{body\ in\ ECEF} \end{bmatrix} \tag{10}$$

The first three elements of X_{RV} provide the position of the RV in ECEF coordinates. Applying Borkowski's Iterative Method yields the latitude, longitude, and elevation of the RV.

The last three elements (4,5,6) of X_{RV} provide the velocity of the RV in ECEF coordinates. The RV speed can be computed with Equation 11.

$$Speed_{RV} = sqrt(X_{RV}(4)^2 + X_{RV}(5)^2 + X_{RV}(6)^2) \tag{11}$$

The RV heading represented in the ENU frame can be computed by rotating the RV velocity vector as shown in Equation 12.

$$RV\ ENU\ heading = (R_{ENU\ to\ ECEF})^{-1} * X_{RV}(4{:}6) \tag{12}$$

Using the inverse tangent function, this can be converted into an angle representation of the RV's heading.

Algorithm Development for a Realistic System

In an ideal system, measurements would be made across all variables of interest at the same time. Figure 9 shows the times at which samples were collected in a realistic system. These data were collected during testing on the Virginia Smart Road. The data were not uniformly sampled at the same time, which would be problematic for the algorithm developed for an ideal system. If the ideal system algorithm were implemented on a system with a realistic data sampling scheme, the majority of generated BSMs would be very inaccurate. For example, if the GHV is traveling at a constant 60 mph and its position is sampled at t = 1887.6 s, this position would be inaccurate by 24 m at t = 1888.5 s, which is 0.1 seconds before the GHV's position is sampled again.

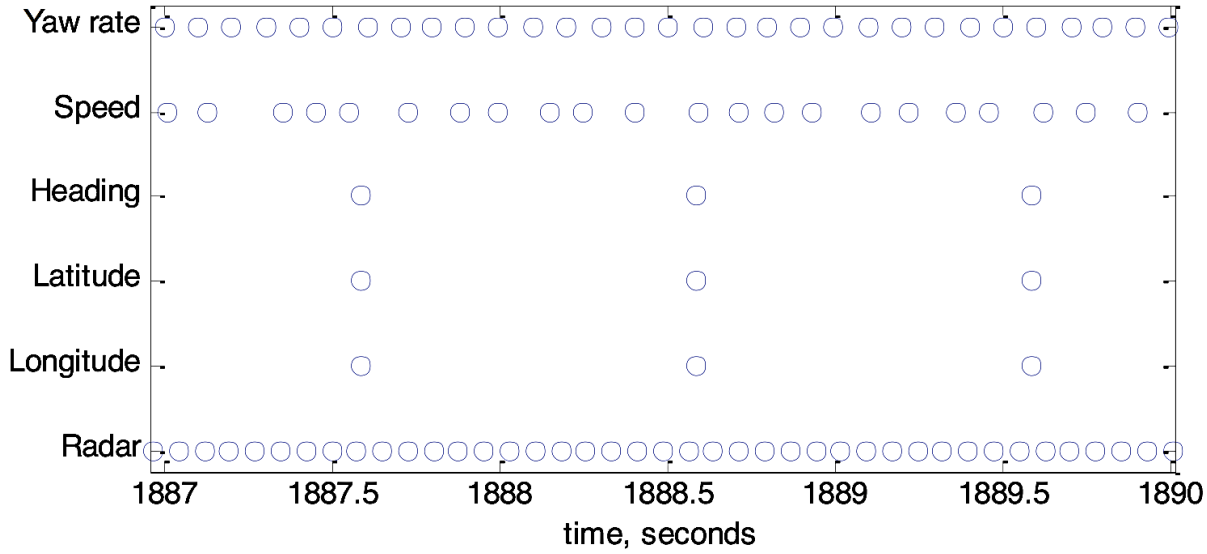

Figure 9. Times at which measurements are made onboard the GHV.

To improve accuracy of computed RV position, better estimates of GHV heading and position at all points in time are needed. For example, the GHV's heading can be estimated at any point in time with Equation 13.

$$\theta(t + dt) = \theta(t) + \dot{\theta}(t) * dt \tag{13}$$

The kinematic state of the GHV can be estimated at any point in time with Equation 14. The vehicle state needs to be updated frequently in order to account for changes in the GHV's speed and heading. New measurements of the GHV's position and speed and new estimates of heading are incorporated into the estimated vehicle state via a Kalman filter.

$$X_{HV}(t + dt) = \begin{bmatrix} 1 & 0 & 0 & dt & 0 & 0 \\ 0 & 1 & 0 & 0 & dt & 0 \\ 0 & 0 & 1 & 0 & 0 & dt \\ 0 & 0 & 0 & 1 & 0 & 0 \\ 0 & 0 & 0 & 0 & 1 & 0 \\ 0 & 0 & 0 & 0 & 0 & 1 \end{bmatrix} X_{HV}(t) \tag{14}$$

Vehicle System Development and Integration

The research team coordinated with the Center for Technology Development (CTD) at the Virginia Tech Transportation Institute (VTTI) to identify, develop, source, and procure the hardware and software components necessary to dynamically generate target vehicle data.

Provided below is a summary of the hardware and software required.

GHV and RV Hardware

- In-vehicle application computer (algorithm running system)
- VTTI data acquisition system (DAS)
- Inertial measurement unit (IMU)
- Forward radar
- Onboard equipment (OBE) (Dedicated Short Range Communications [DSRC] radio)

Software

- Application Program Interface (API) allowing access to real-time data from GPS, IMU, and ranging sensor to application computer for algorithm
- Application computer transmitting algorithm output to DAS to support performance analysis
- Application computer transmitting algorithm output to OBE for message generation and OTA transmission

The BSM provides a standardized structure for transmitting data elements such as those generated by the algorithm developed for this project. A system was developed to feed sensor data from a forward facing radar, GPS, and IMU into an algorithm that would produce elements in a BSM. The data output of the algorithm interfaced with the DSRC onboard unit (OBU) for transmission OTA to other CVs and infrastructure. Additionally, the output of that data from all sensors was captured by the VTTI DAS for post-test assessment of the algorithm. The details of that system are provided in Figure 10 below.

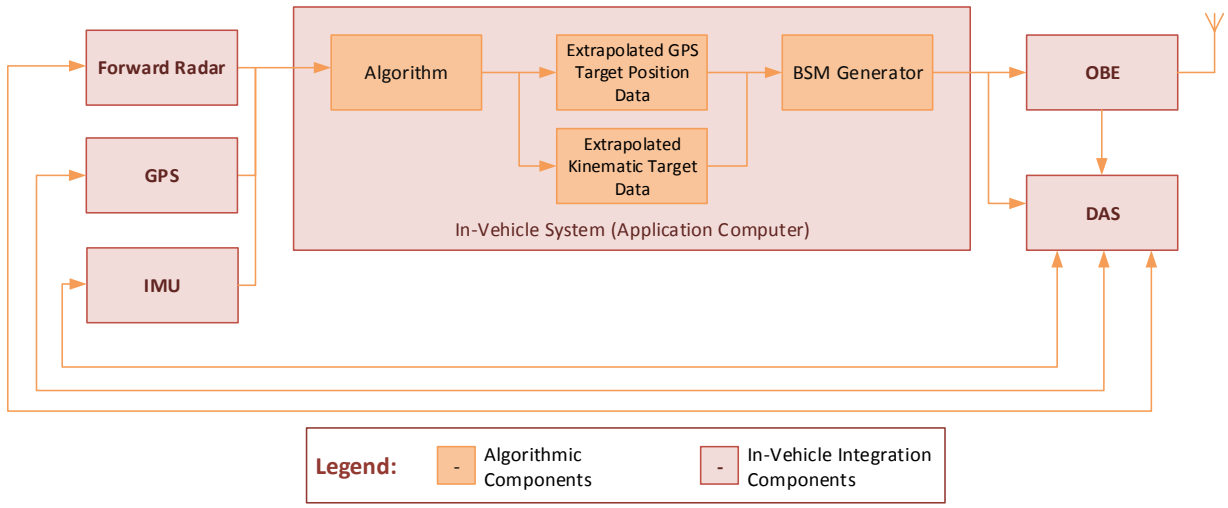

Figure 10. System diagram.

The system described above was installed in two vehicles, a white Chevy Tahoe and silver Infiniti M35. Both vehicles were developed to generate and log BSMs for targets detected by radar. In order to assess the performance of the algorithm, however, the two vehicles were tested against each other, with one vehicle functioning as the GHV and the other as the RV in predefined configurations. Since the data collected by the DAS included the actual BSM from the RV, it was possible to compare the pseudo BSM (representing the RV) generated by the GHV against the BSM broadcast from the RV to assess performance. The performance variables specifically of interest were the RV latitude, longitude, heading, elevation and speed elements.

A Savari MobiWAVE vehicle awareness device (VAD; see specifications in Savari, 2012) was used in testing. An embedded GPS receiver in the VAD populates specific data elements in a standardized SAE 2735 DSRC BSM, as shown in Table 2 (SAE International, 2009). The VAD then uses the DSRC radio to transmit the BSMs wirelessly at a rate of 10 Hz (while also receiving BSMs from RVs) via a Hirschmann shark fin combined DSRC/GPS antenna (Figure 11).

Table 1. OBE Technical Specifications (Savari, 2012)

Device	Power	Wireless	GPS	Port	Antenna	Storage
VAD	12-V DC USCAR connector	1 25 dbm DSRC/Wi-Fi 5.15-5.9 GHz, 10, 20 MHz channels, 802.11a	±2 m position accuracy, 50% CEP	1 Ethernet 1 RS-232 2 USB 2 FAKRA	Multiband Wi-Fi/ DSRC/ GPS	Up to 512 MB internal, USB external

Table 2. BSM Data Elements (SAE International, 2009)

Dynamic Content		Static Content
DSRC Message ID	Positional Accuracy	Vehicle Width
Message Count	Heading	Vehicle Length
Temporary ID	Transmission and Speed	Vehicle Height
Dsecond	Steering Wheel Angle	Vehicle Type
Latitude	Acceleration Set (Four Way)	
Longitude	Brake System Status	
Elevation	Event Flag	

Figure 11. Hirschmann shark fin combined DSRC/GPS antenna.

Experimental Test Development and Execution

Various experimental tests were developed to test the performance of the algorithmically generated BSM elements versus the actual BSM for various vehicle formations, traffic densities, velocities, and roadway environments and features. Experiments were conducted on the Virginia Smart Road and on real-world roads in the New River Valley of Virginia.

Smart Road Testing

A series of tests were conducted on the Virginia Smart Road, a 2.2-mi controlled-access test bed managed by VTTI in Blacksburg, Virginia. The Smart Road offers a variety of terrain, CV communications, and a differential GPS base station for precise vehicle location.

Static Dwell Test

A static dwell test was designed to assess the algorithm's performance in a static environment where GPS values would likely drift within a known Circular Error Probable (CEP) range as defined by the GPS data sheet. Considering that the algorithm uses the GHV's GPS position to generate the RV's GPS position, it is of interest to understand the change of GPS location and its effects on the algorithm.

The static dwell test was conducted on a straight and level portion of the Smart Road, which is shown in Figure 12.

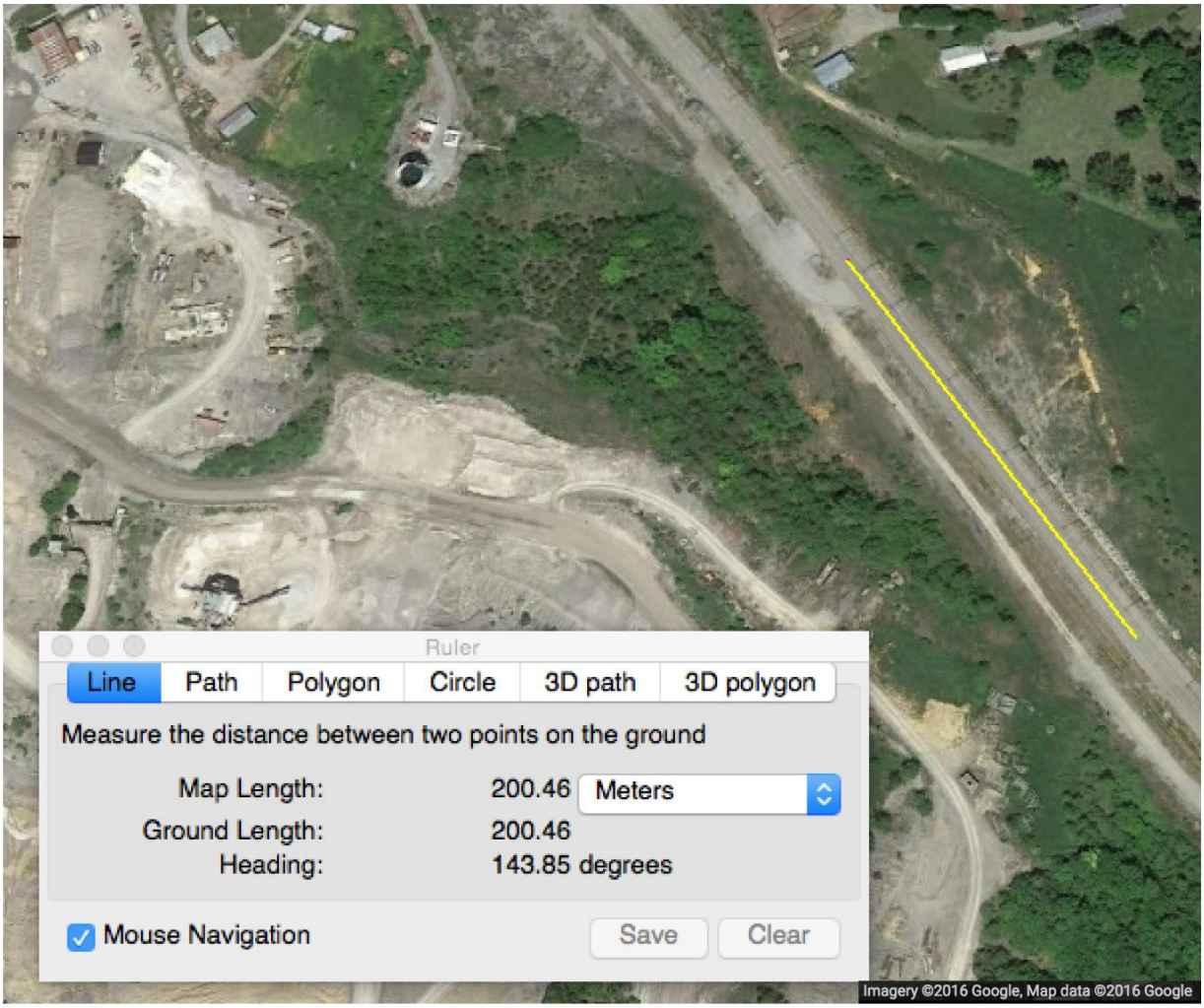

Figure 12. Segment of the Smart Road used for static dwell test.

The static dwell test is illustrated in Figure 13. The procedure used was as follows:

1. The GHV was positioned behind the RV in the same lane, centerline of the lane and offset by predefined distances on the roadway.

2. The distance from the GHV's front bumper to the RV's rear bumper was set at the following distances: 5 m, 10 m, 30 m, and 60 m.

3. The vehicles dwelt at each range position for 2 minutes.

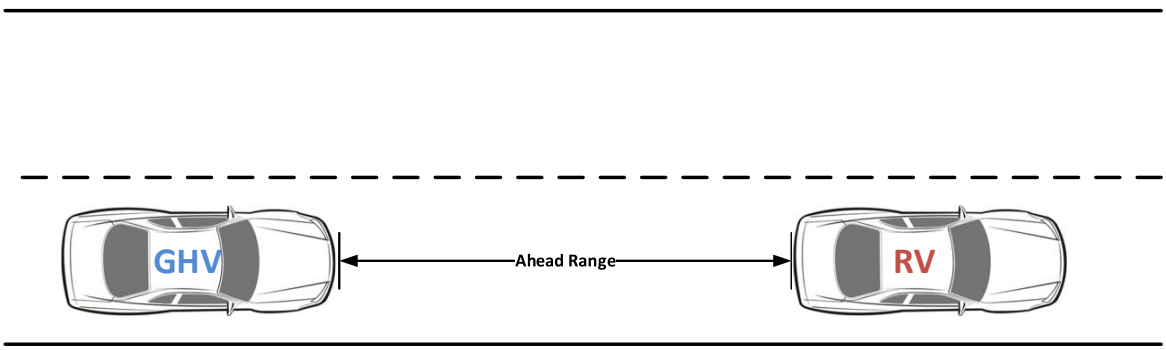

Figure 13. Static dwell test.

Dynamic Ranging

The dynamic ranging test assessed the algorithm's performance in a dynamic environment, in which the GHV generated a BSM for an RV that drove away in lane until out of radar range, turned around, and drove toward and past the GHV in an adjacent lane. It is of interest to understand the effects of the algorithm's performance in terms of the relative range between vehicles, especially at the fringes of radar detection.

The dynamic ranging test was conducted on a straight and level portion of the Smart Road that allows for easy U-turning (depicted in Figure 14).

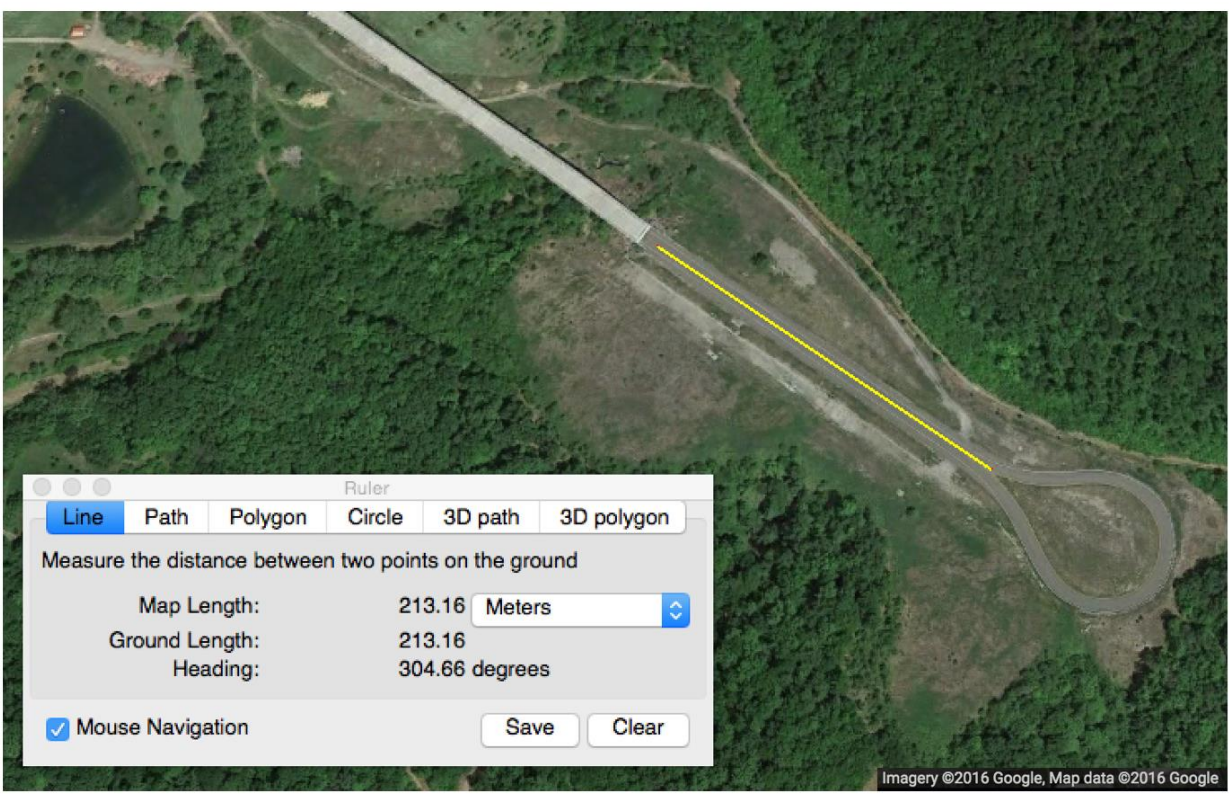

Figure 14. Segment of the Smart Road used for dynamic ranging test.

The dynamic ranging test is illustrated in Figure 15. The procedure used was as follows:

1. The GHV was positioned approximately 5 m behind the RV in the same lane, centerline of the lane on the road.
2. While the GHV remained parked, the RV drove away in the same lane for approximately 200 m. By design, the RV was to accelerate quickly until it reached its target speed and hold the target speed as long as it can do so safely.
3. Upon reaching 200 m, the RV turned around and drove in the adjacent lane toward the GHV. After turning around, the RV accelerated back up to the target speed.
4. Steps 1–3 were repeated for three attempts for four different RV target speeds (total of 12 attempts). The target speeds were 10 mph, 20 mph, 35 mph, and 55 mph.

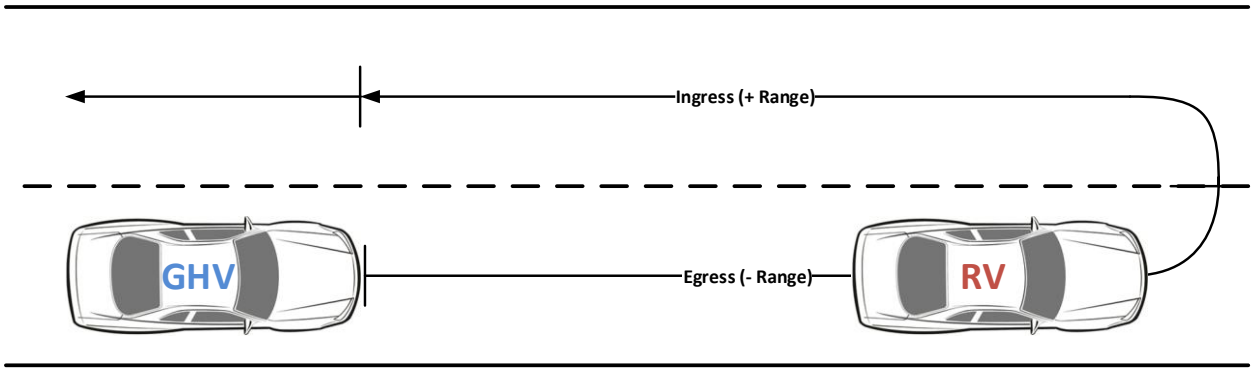

Figure 15. Dynamic ranging test.

Dynamic Platoon

The dynamic platoon test assessed the performance of the GHV to generate BSMs for an RV located ahead of the GHV in a dynamic environment on the Smart Road. The Smart Road provides curved roadways, open sky, and mountainous terrain that may impact the performance of the algorithm. The data collected on the GHV following the RV on the Smart Road facilitated analysis of the impacts of environmental features on the algorithm.

The entire Smart Road was used for the dynamic platoon test (depicted in Figure 16).

Figure 16. Smart Road course for dynamic platoon test.

The dynamic platoon test is illustrated in Figure 17. The procedure for the dynamic platoon test was as follows:

1. The GHV was positioned behind the RV in the same lane, centerline of the lane on the road.

2. The RV and GHV were driven in their starting formation, with the GHV trailing the RV. A constant, safe following distance was maintained between the vehicles throughout the test.

3. The test continued for five loops around the Smart Road.

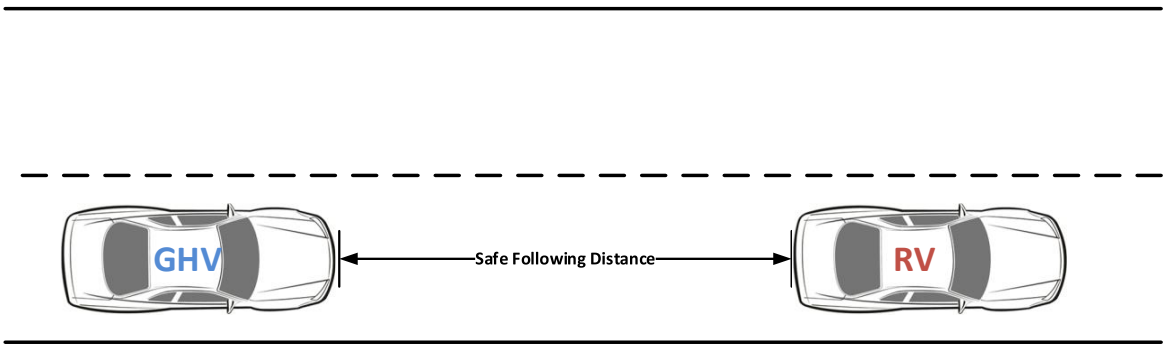

Figure 17. Dynamic platoon test.

Dynamic Maneuvering

Three dynamic maneuvering tests were conducted: RV ahead cut-in, RV acceleration/deceleration, and RV overtake. These tests assessed the performance of the GHV to generate BSMs for an RV located ahead in several maneuvers that are indicative of crash scenarios. The entire Smart Road was used for these tests.

RV Ahead Cut-In

Figure 18 illustrates the RV ahead cut-in scenario. The procedure for the test was as follows:

1. The GHV was positioned behind the RV in the same lane, centerline of the lane on the road.
2. The vehicles began driving and maintained a constant, safe following distance between them at 30 mph.
3. The GHV stayed in the lane while the RV changed into the adjacent lane and then returned into the GHV's lane (see Figure 18).
4. The procedure was repeated for five laps of the Smart Road.

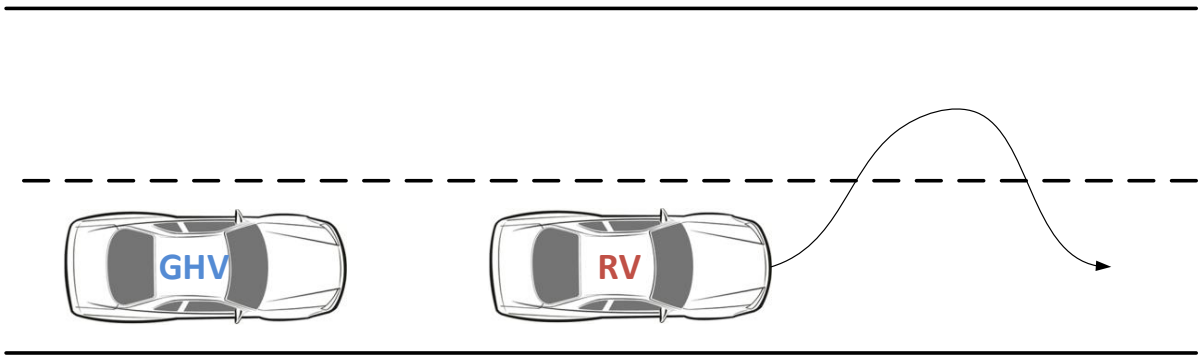

Figure 18. RV ahead cut-in scenario.

RV Acceleration/Deceleration

Figure 19 illustrates the scenario for the RV acceleration/deceleration test. The procedure for the test was as follows:

1. The GHV was positioned behind the RV in the same lane, centerline of the lane on the road.
2. The vehicles began driving and maintained a constant, safe following distance between them at 30 mph.
3. As the GHV stayed in lane, the RV accelerated to a speed of 60 mph and maintained that speed in the same lane as the GHV. (Note: The GHV and RV had plenty of distance between them to avoid a collision.)
4. The RV braked and came to a complete stop.
5. The GHV began braking at a safe distance and came to a complete stop.
6. Steps 2–5 were repeated for five laps of the Smart Road.

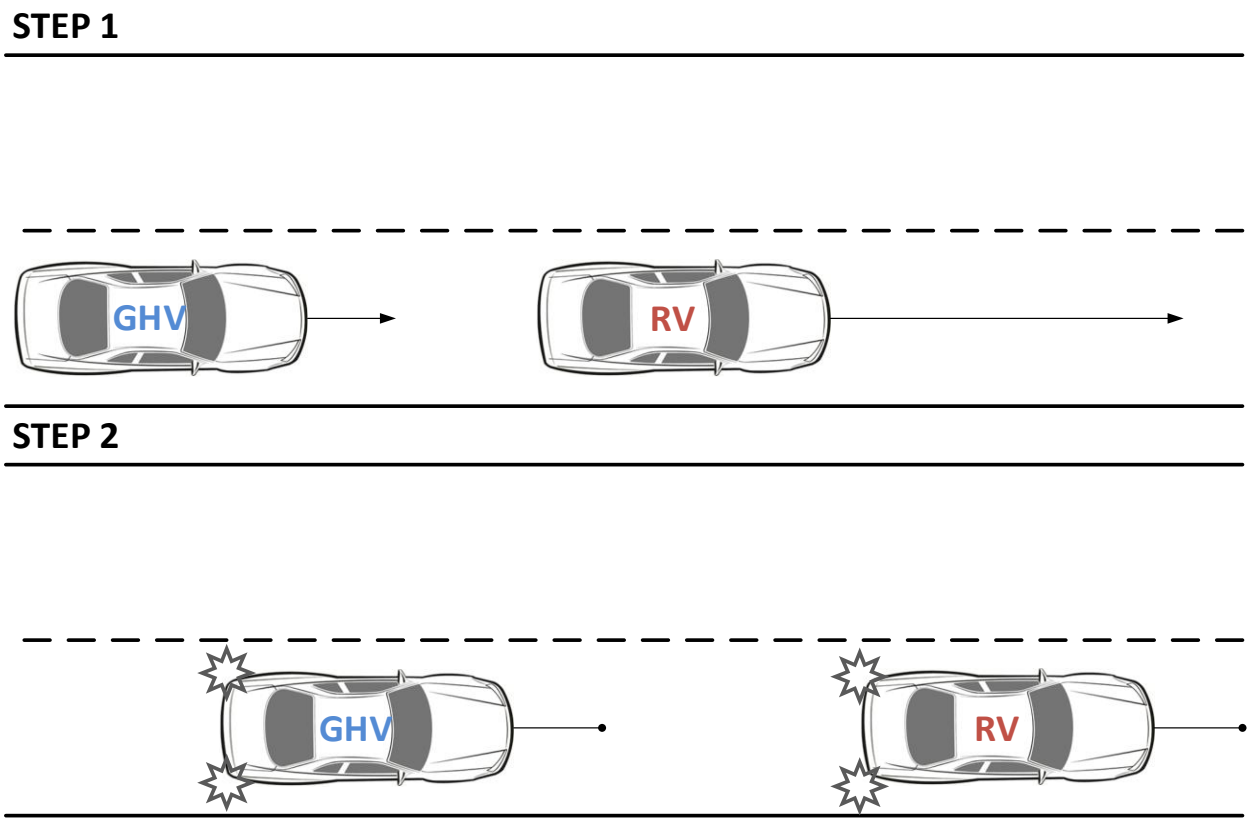

Figure 19. RV acceleration/deceleration test.

RV Overtake

Figure 20 illustrates the scenario for the RV overtake test. The procedure used for this test was as follows:

1. The GHV was positioned slightly ahead of the RV in an adjacent lane (outside radar view). Both vehicles were aligned by their respective centerline of the lane on the road.

2. The vehicles began driving and maintained a constant speed of 30 mph. The RV continued to stay slightly behind the GHV.

3. Once a constant speed was reached, the RV accelerated, passed the GHV by ~200 m, cut in to the GHV's lane, and slowed down.

4. At a safe distance, the GHV cut in to the adjacent lane and passed the RV.

5. After the GHV passed the RV in the adjacent lane, the RV accelerated to stay slightly behind the GHV in the adjacent lane.

6. Steps 2–5 were repeated for a duration of five laps of the Smart Road.

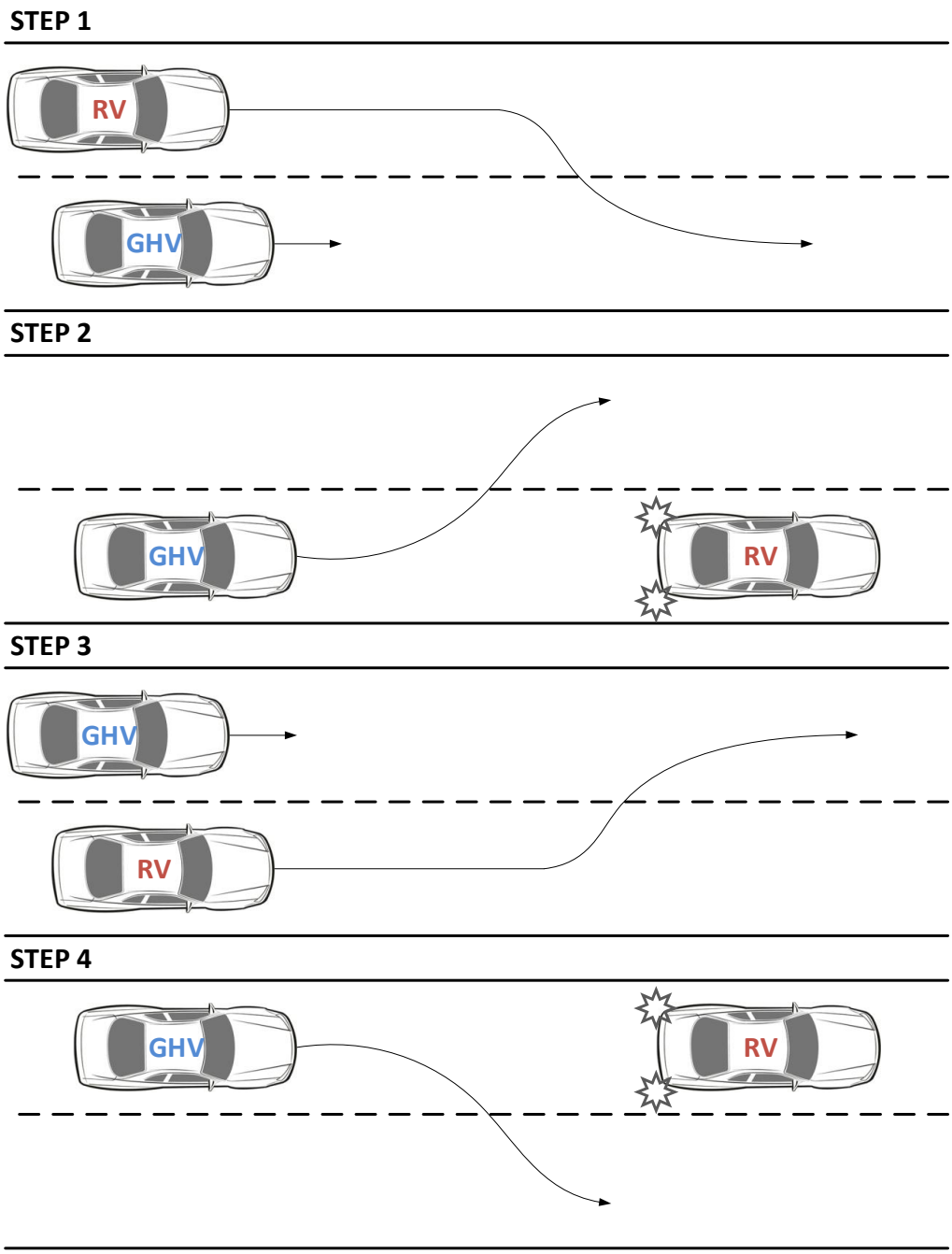

Figure 20. RV overtake test.

Public Road Testing

Public road tests were conducted to collect data in real-world environments. Public road testing provided challenging environments and roadways not found on the Smart Road. In addition, the presence of non-CVs in traffic allows for assessment of how the algorithm would perform when more than one dynamic target was present. During the road testing, the vehicles maintained the same configuration and safety considerations as in the dynamic platoon experiments. To the best

of their ability, the drivers of the GHV and RV also tried to minimize the number of cut-ins by other vehicles and drive in the same lane.

A route was developed that took into account challenging roadway environments in the New River Valley such as mountainous roadways. The route is shown in Figure 21.

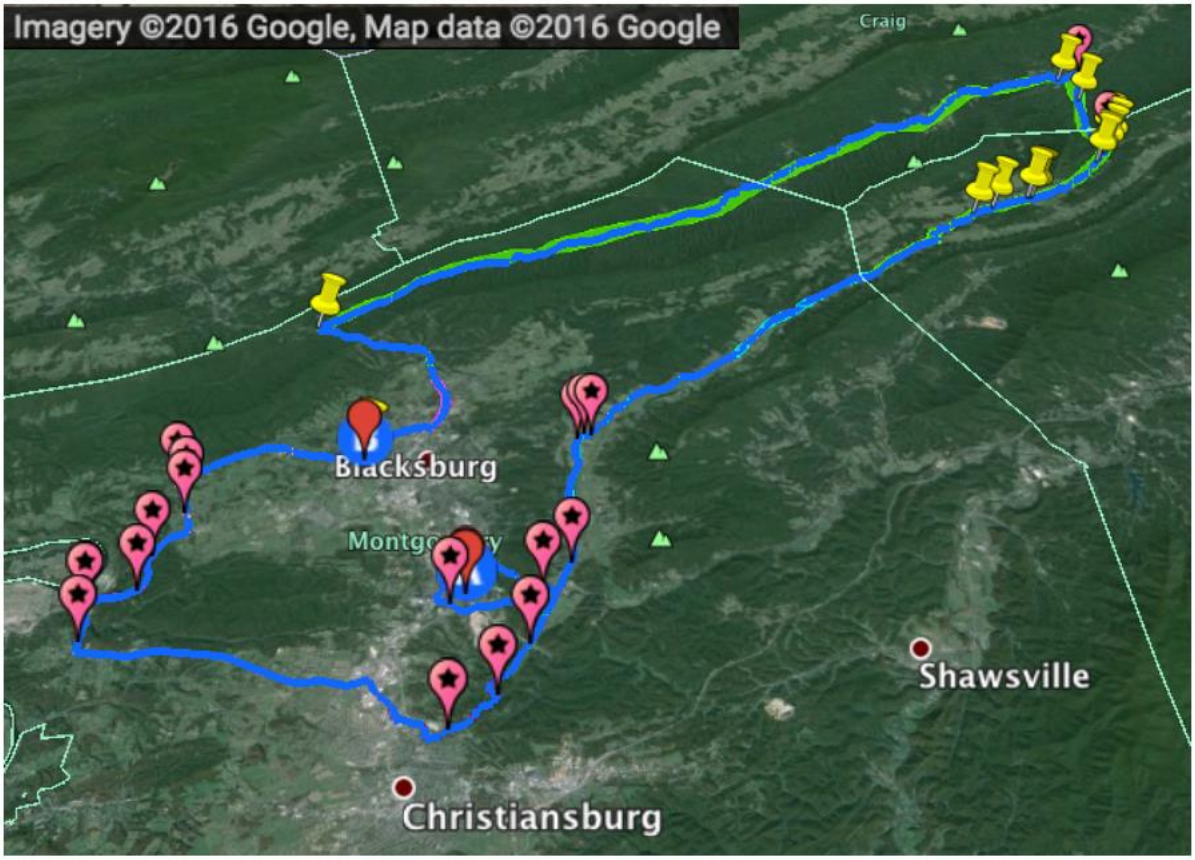

Figure 21. Route used for road testing.

Results

Results discussed within this section are based on the data collected during static dwell, RV acceleration/deceleration, RV ahead cut-in/cut-out, RV overtake, and public road testing.

At the onset, the project team had intended to implement an initial algorithm within the vehicle hardware, capture data via the process described in the Methods section, refine the algorithm based on this data, and then redeploy a refined algorithm in a second set of data collection for further evaluation. Development and integration of the algorithm was more involved than anticipated and consumed resources beyond those initially planned. As such, the team successfully integrated the initial algorithm, collected data, and refined the algorithm; however, the team was not able to contain the second data collection and evaluation within this project. Using the objective data collected, the team was able to iteratively improve the algorithm in software and perform thorough

assessments of the algorithm performance. The results of this effort are described within this section.

Algorithm Development Results for an Ideal System

Recall from the Algorithm Development section that the first step in revising the algorithm was to simulate the algorithm for an ideal system. The data collected during the testing session were converted into an ideal system data set via linear interpolation between data points. Because we focused on real-world data from automotive-grade components, the data were subject to measurement error. Despite measurement inaccuracies, the data provided for a relevant framework for algorithm development.

Figure 22 compares the actual measurements of latitude, longitude, elevation, speed, and heading collected on the RV against the latitude, longitude, elevation, speed, and heading that were estimated for the RV using GHV data. The thick black line corresponds to the actual RV measurements. The colored dots correspond to estimates made with GHV data. Each color represents a different radar target as indicated by the radar Object_ID. At first glance, the actual measurements seem to align well with the estimated values. Notable exceptions include targets with a speed close to zero. These measurements are of stationary objects (e.g., guardrails) and were ignored in further algorithm evaluation. The colors used in this plot will be used in future plots to represent the same radar targets. The purpose of identifying the different targets is to visually isolate outliers that are likely coming from a source other than the RV.

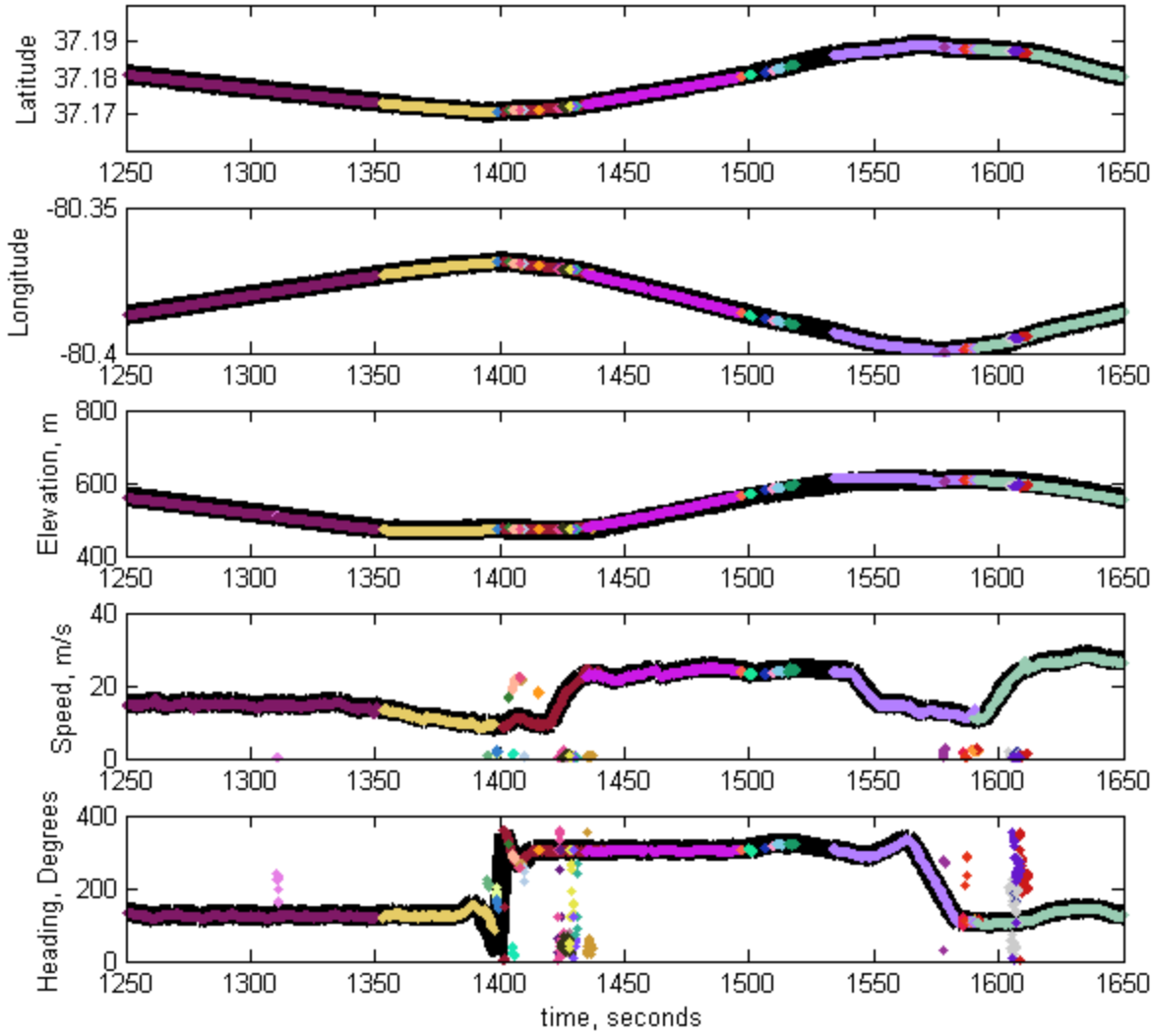

Figure 22. Comparison of actual RV measures against estimated RV measures.

Figure 23 shows the difference between actual RV measures and the estimated values computed with GHV data. Radar targets with speeds less than 10 mph were assumed to be stationary and were excluded from this plot. The Euclidean distance between RV GPS measurements and the estimated RV position shows a disagreement usually exceeding 5 m. The actual speed and estimated speed are very much in agreement, with a difference usually less than 1 m/s. The disagreement in RV position is likely due to GHV radar, GHV GPS, RV GPS, or GHV heading bias/error. The RV heading measurements are in agreement except when the vehicles were traversing curves, which means they were not traveling with the same heading at the same time.

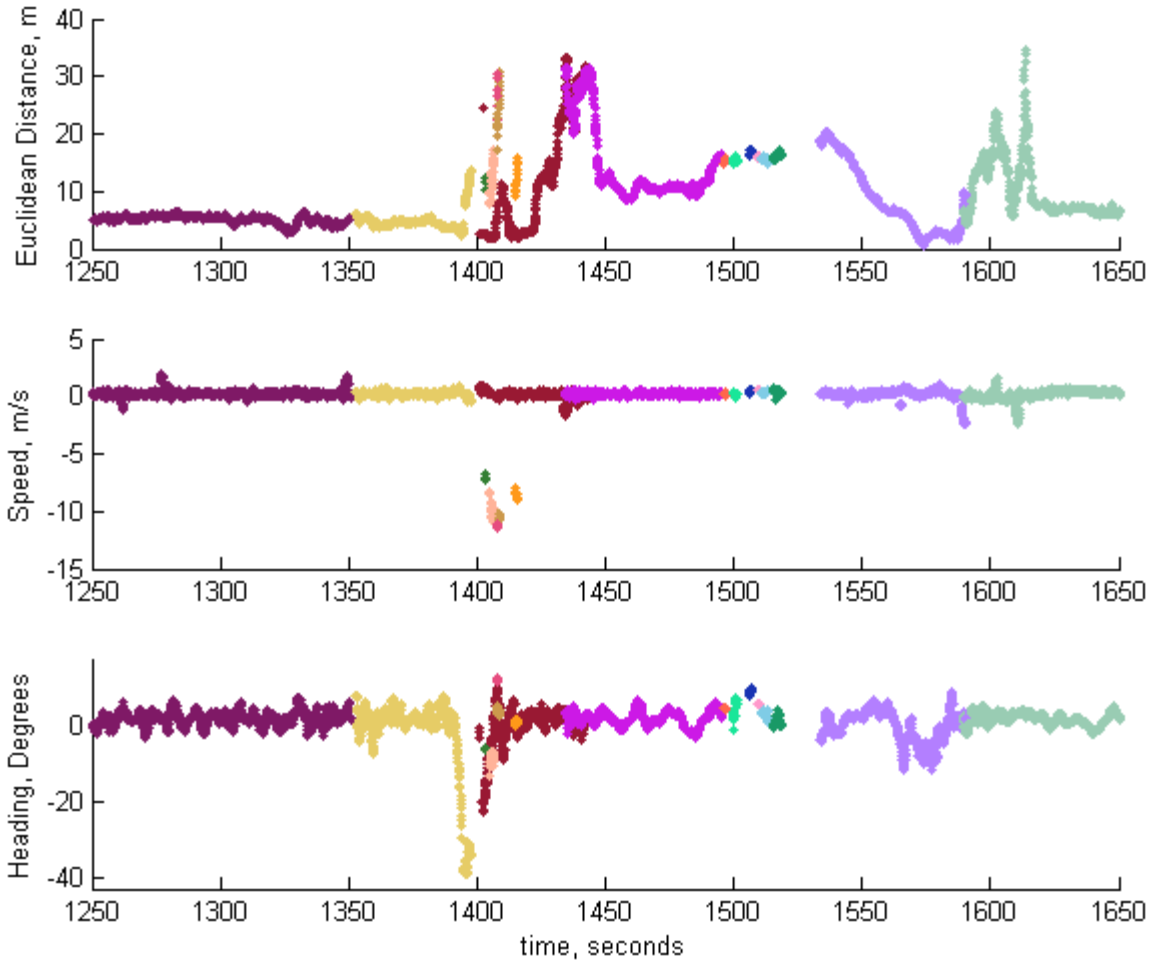

Figure 23. Difference between actual RV measures and estimated RV measures.

In order to better understand the potential sources of disagreement between measured and estimated RV position, the differences between values were projected onto the axes of the GHV body-fixed coordinate system. Figure 24 shows the Euclidean distances (in meters) between measured and estimated positions, projected onto the *x*-axis, *y*-axis, and *z*-axis (ref. Figure 7) of the GHV body-fixed coordinate system. It is immediately apparent that a large source of estimation error stems from the inability of the algorithm to correctly estimate the RV's elevation. This makes sense because the algorithm does not estimate the vertical offset. Since this cannot be measured directly (i.e. the radar does not measure along the z-axis), vertical offset would have to be estimated by taking into account the pitch of the GHV; however, pitch is not available on many vehicle platforms. Fortunately, error along the z-axis may be of least importance since it is generally only needed to ensure that vehicles are not on two different roadway elevations (e.g. overpass). It is also important to note that tests were conducted on a segment of road with a grade that ranged between 2% and 6%. If tests were conducted on a flat road, the z-axis errors would be minimal.

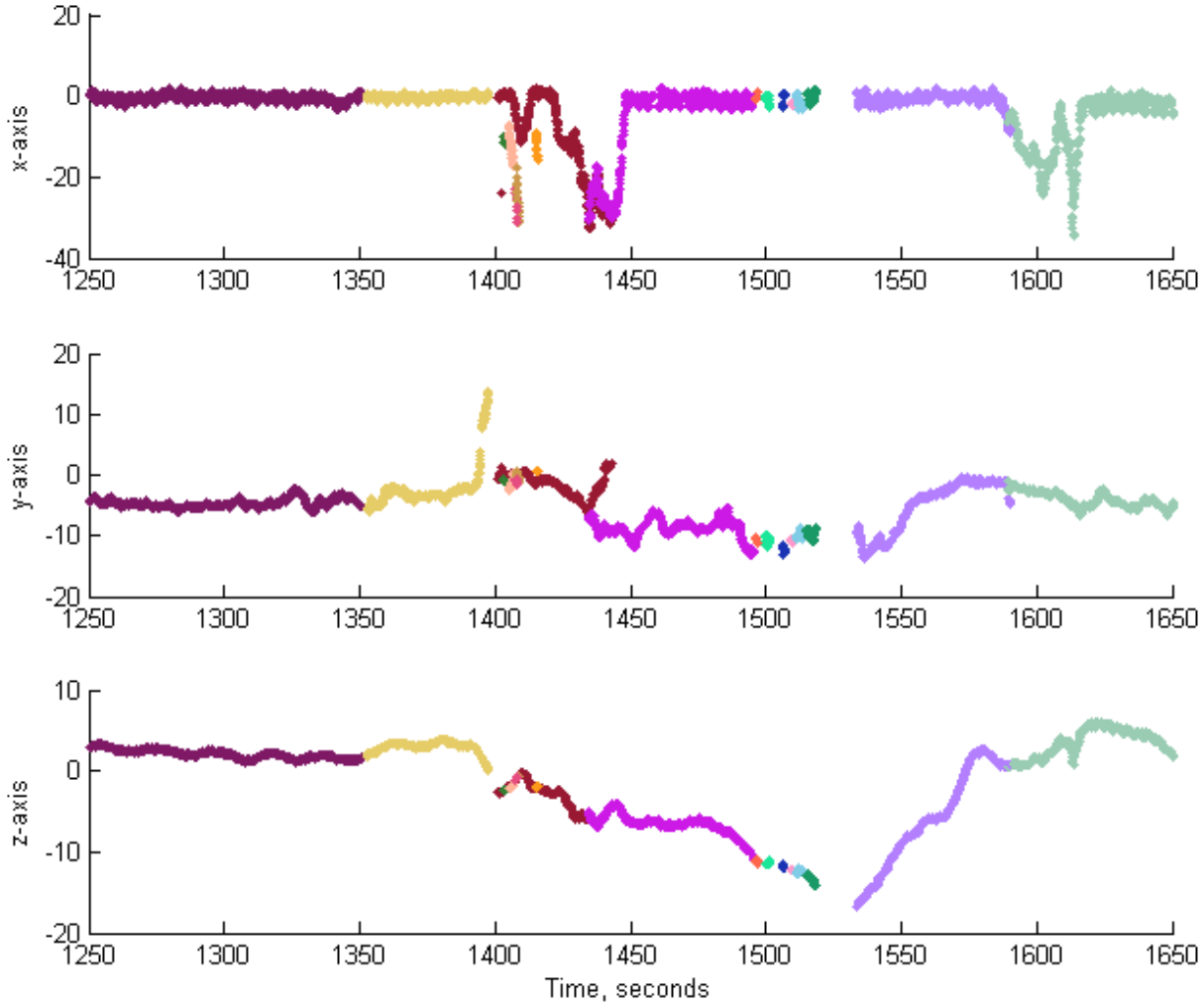

Figure 24. Euclidean distances (in meters) between measured and estimated RV positions, projected onto axes of the GHV body-fixed coordinate system plotted against time.

Figure 25 shows histograms of the data that were presented in Figure 24. If the data were being collected with absolute accuracy and the algorithm were functioning perfectly, we would expect to see modes of zero for all three fixed-body axes. Instead, there are consistent errors for all three axes. Only 9.0% of the RV position estimates were within 3 m of the measured position along the *x*-axis and within 1.5 m of the measured position along the *y*-axis. The values of 3 m and 1.5 m were chosen to reflect position estimates that would not confuse one remote vehicle with another. A value of 3 m was chosen because most ground vehicles have a length from rear bumper to front bumper of at least 3 m. A value of 1.5 m was chosen because most ground vehicles have a width of at least 1.5 m.

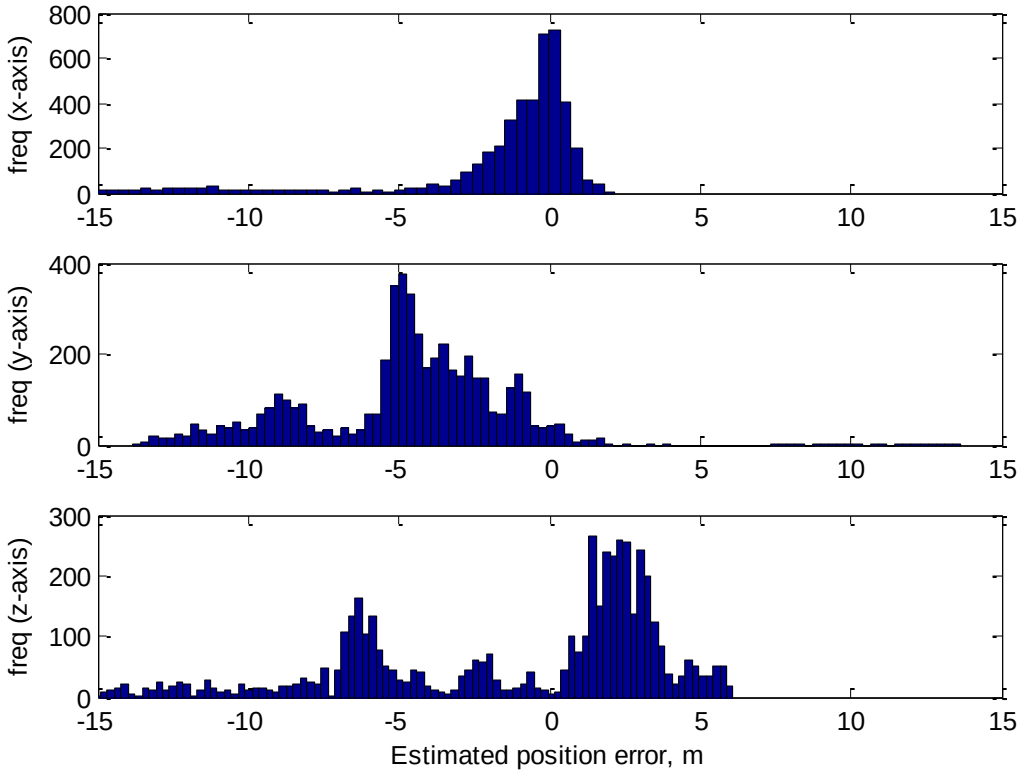

Figure 25. Frequencies of binned Euclidean distances (in meters) between measured and estimated RV positions, projected onto axes of the GHV body-fixed coordinate system.

Figure 26 shows the Euclidean distances (in meters) between measured and estimated positions, projected onto the *x*-axis, *y*-axis, and *z*-axis of the GHV body-fixed coordinate system plotted against the GHV measured radar range. These plots show that as the distance between vehicles increases, the difference between position estimates and measurements increases. The reason for these trends in the z-axis can mostly likely be attributed to the grade of the road on which tests were conducted and the fact that the algorithm does not take into account any vertical offsets. Future algorithms would account for vertical offsets by estimating the pitch of the GHV. The reason for these trends in the y-axis can most likely be attributed to a misaligned radar system.

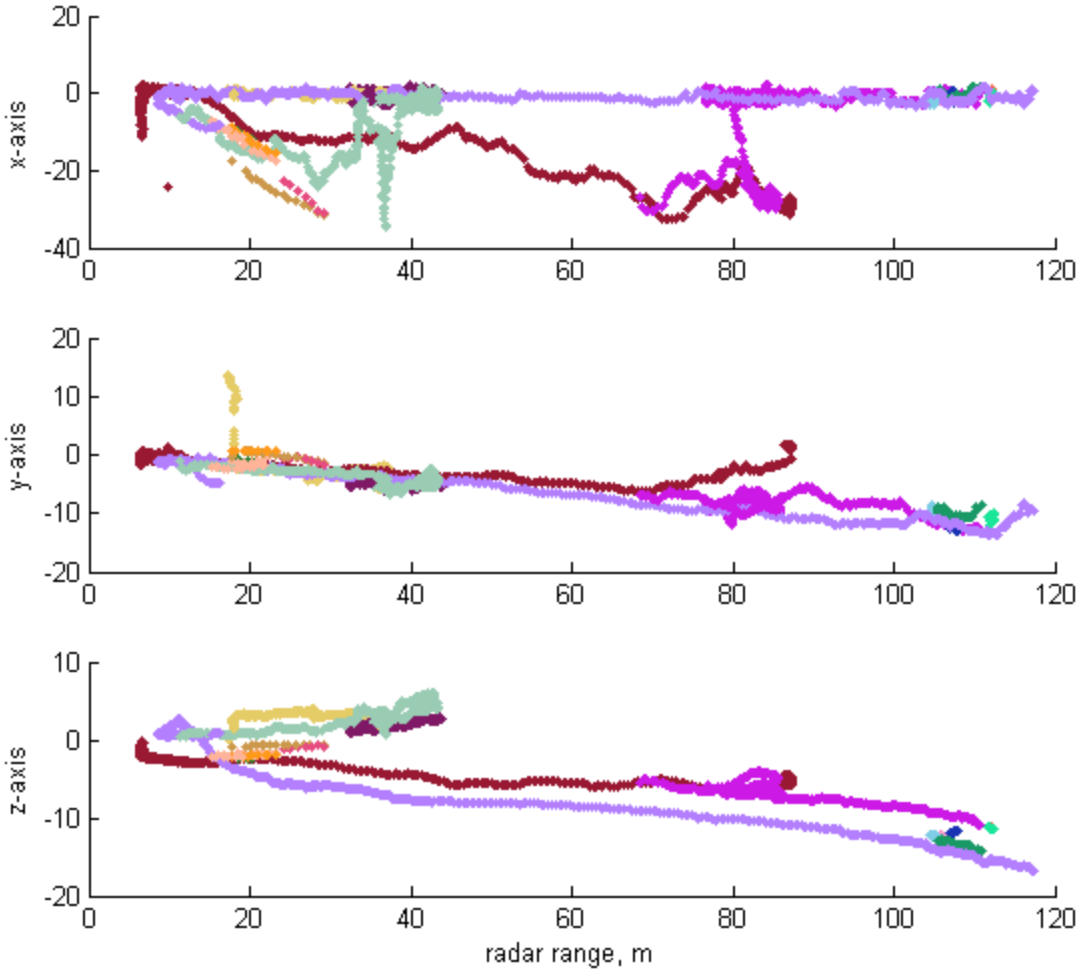

Figure 26. Euclidean distances (in meters) between measured and estimated positions, projected onto the *x*-axis, *y*-axis, and *z*-axis of the GHV body-fixed coordinate system plotted against the GHV measured radar range.

Figure 27 shows estimates for the degree to which the radar system was misaligned. Ideally, the angle between the plane of the radar system and the plane of the GHV front bumper should be zero degrees. However, this figure indicates that the angle between these two planes has a magnitude greater than 5 degrees.

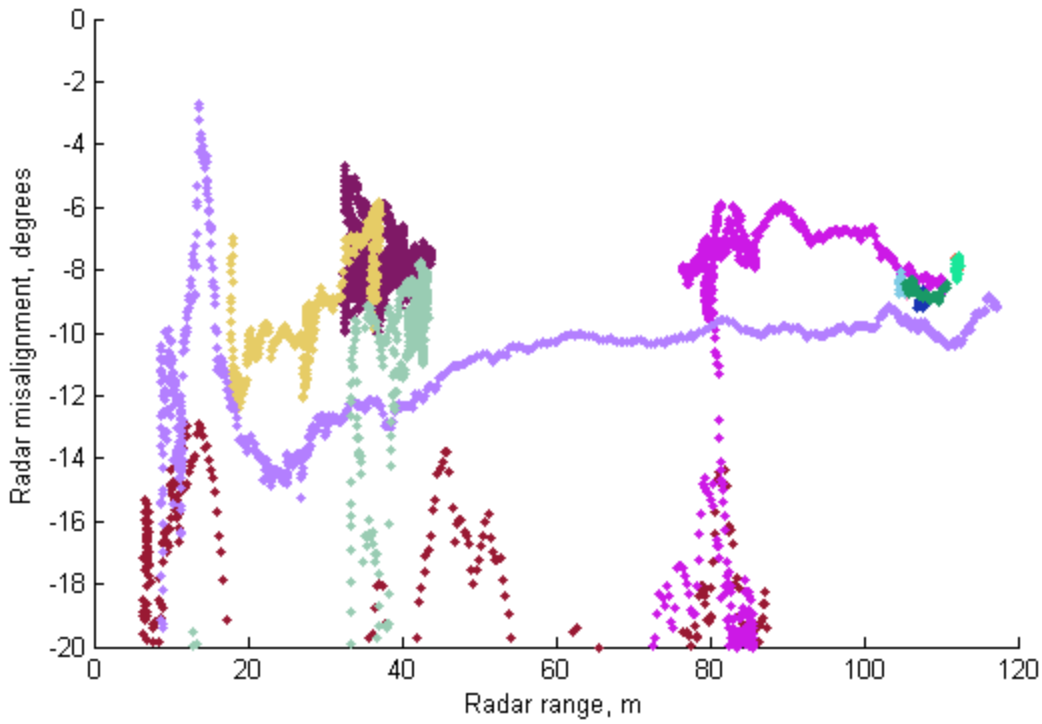

Figure 27. Estimates for radar misalignment as a function of radar range.

After improving the algorithm to account for a misaligned radar system, the algorithm was executed again on the same data set. Figure 28 shows the histograms of Euclidean distances between the measured and estimated RV positions, projected onto the axes of the GHV body-fixed coordinate system. This figure shows a great improvement in the algorithm's ability to accurately estimate an RV's position. The percentage of RV position estimates that were within 3 m of the measured position along the *x*-axis and within 1.5 m of the measured position along the *y*-axis improved from 9.0% to 67.9%. According to SAE standards, a BSM should report speed with 1 km/h accuracy for 68% of test measurements. Our algorithm was able to report speed with this accuracy for 57.8% of test measurements. According to SAE standards, when a vehicle is traveling above 45 km/h a BSM should report heading with 2 degrees accuracy for 68% of test measurements. Our algorithm was able to report heading with this accuracy for 45.9% of test measurements.

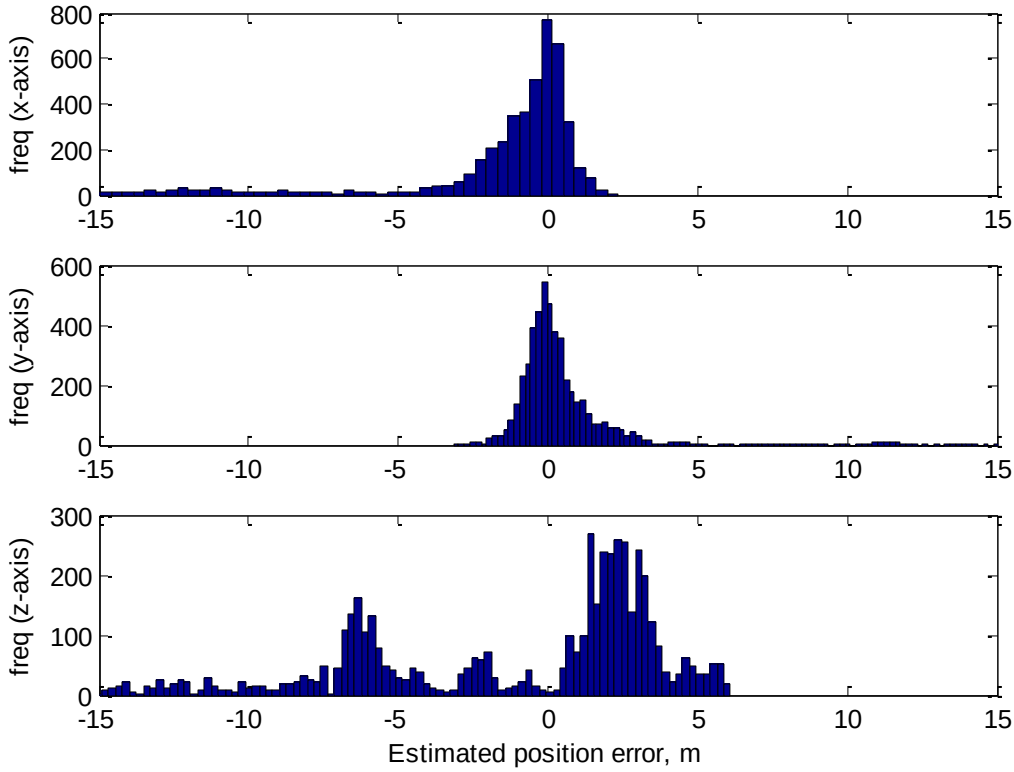

Figure 28. Frequencies of binned Euclidean distances (after radar misalignment correction) between measured and estimated RV positions, projected onto axes of the GHV body-fixed coordinate system.

Discussion

The final results showed that 67.9% of the RV position estimates were within 3 m of the measured position along the *x*-axis and within 1.5 m of the measured position along the *y*-axis. These values of 3 m and 1.5 m were chosen to reflect position estimates of one RV that could not be confused with another RV. The RV speed and heading estimates were able to meet SAE J2945/1 standards 57.8% of the time and 45.9% of the time, respectively.

If the radar system had been aligned perfectly before testing, perhaps the success rate would have been higher; however, the post-hoc alignment procedure should have corrected for the majority of alignment errors. Another source of error may be inherent inaccuracies with the current version of the radar system. Without this tendency, RV position estimates could be further improved as a whole. Other possible methods of improving RV position estimates would be to fuse the radar data with additional sensors to improve measurement accuracy, such as camera-based vision data, Lidar, or perhaps a more accurate GPS.

Given the limited resources, the small research team was able to contribute a great deal to CV research. The team was able to develop an algorithm that can estimate an RV's heading and speed with excellent success and can estimate the RV's position with moderate success. During

algorithm development, the researchers gained insight into the limitations of the GHV sensors and discovered the need for sensors less prone to error and/or bias. The research team successfully integrated the algorithm into the vehicle's system and demonstrated the ability to send BSMs (albeit erroneous ones due to a bug in the algorithm at the time) on behalf of an RV.

Conclusions and Recommendations

This project was able to meet its objective of developing an in-vehicle technical implementation to generate the GPS position, speed, and heading of a radar-detected vehicle for use in OTA communications such as the BSM. Due to resource constraints, the team was unable to deploy an improved system for a second round of testing and data collection. Based on analysis discussed in the previous section, implementation of the improved algorithm as well as updated operating procedures would produce markedly improved results. It is the desire of this team, if given additional resources, to execute a developmental cycle in which multiple rounds of testing and algorithmic improvement iterations are executed. The end goal of such an endeavor would be to produce a system that generates BSMs for target vehicles that are just as reliable as BSMs transmitted from an OBE.

Although this project focused on generating and populating BSM Part I elements, integration into BSM Part II or other OTA messages should be considered. Consider the Cooperative Adaptive Cruise Control (CACC) project, an ongoing intelligent transportation system (ITS) research project. The CACC project is investigating an extension of Adaptive Cruise Control (ACC) systems to dynamically and automatically coordinate a string of vehicles in order to improve traffic flow (Parikh et al., 2015). The CACC study has assessed the potential benefits of augmenting production-level radar-based ACC systems with DSRC, which may include possible flow stabilization and reductions in headway resulting from improved information exchange between vehicles (Parikh et al., 2015). It was determined that vehicle-to-vehicle (V2V) BSM communication may or may not have sufficient information to support CACC operation without additional information from onboard sensors (Parikh et al., 2015). Based on this finding, the report recommends investigating the need for additional messages and data elements.

The benefits of utilizing ranging sensor data may not only complement V2V but could also be used to enhance vehicle-to-infrastructure (V2I) systems to support mobility applications. Considering that such sensors can be used to assess the number of targets, relative locations, and speeds, a wide range of insights could be gained to support traffic operations. Such data could help to characterize the local roadway environment in terms of dynamic traffic density and flow. Furthermore, interactions between vehicles in terms of following distances could be extracted to detect crashes and near-crashes. Complementing vehicle position and speed with kinematic interactions between vehicles would enrich the data, allowing for the realization of new applications.

References

Burtch, R. (2006, April 21-26). *A comparison of methods used in rectangular to geodetic coordinate transformations.* Paper presented at ACSM Conference and Technology Exhibition, Orland, FL. Retrieved from http://citeseerx.ist.psu.edu/viewdoc/download?doi=10.1.1.139.7504&rep=rep1&type=pdf

National Highway Traffic Safety Administration. (2006). *Vehicle survivability and travel mileage schedules* (DOT HS 809 952). Retrieved from https://crashstats.nhtsa.dot.gov/Api/Public/ViewPublication/809952

Parikh, J., Abuchaar, O., Haidar, E., Kailas, A., Krishnan, H., Nakajima, H., . . . Deering, R. (2015). *Cooperative Adaptive Cruise Control (CACC) final report* (FHWA-JPO-16-257).Washington, DC: Federal Highway Administration.

SAE International. (2009). *SAE J2735 Surface Vehicle Standard - Dedicated Short Range Communication (DSRC) Message Set Dictionary*. Warrendale, PA: Author.

Savari. (2012). MobiWAVE on board equipment. Retrieved from http://www.savarinetworks.com/files/MobiWAVE-DS-Family.pdf